Appl Biol Chem (2016) 59(2):181–192
DOI 10.1007/s13765-016-0148-9

Online ISSN 2468-0842
Print ISSN 2468-0834

ARTICLE

Biological features, drug-likeness, pharmacokinetic properties, and docking of 2-arylidenehydrazinyl-4-arylthiazole analogues

Mohammad Sayed Alam[1] · **Junaid Uddin Ahmed**[2] · **Dong-Ung Lee**[1]

Received: 12 October 2015 / Accepted: 12 November 2015 / Published online: 29 January 2016

Abstract Thiazoles are an important class of heterocyclic compounds that possess a sulfur and nitrogen containing five-membered ring, which acts as a pharmacophore, and show a wide range of complex biological activities. A series of sixteen 2-arylidenehydrazinyl-4-arylthiazole analogues (**3a–p**) were evaluated for cytotoxic activity against brine shrimp (*Artemia salina*) nauplii and their minimum inhibitory concentrations were determined against two Gram-positive (*Listeria monocytogenes* and *Enterococcus faecalis*) and two Gram-negative bacterial strains (*C. sakazakii* and *E. coli*). Of the tested compounds, **3g** demonstrated highest cytotoxicity with a LC_{50} value of 54 ppm followed by compound **3h** (LC_{50} = 85 ppm), in a short-term bioassay using *A. salina*, whereas compound **3i** exhibited the most potent antibacterial activities against *L. monocytogenes*, *E. faecalis*, and *C. sakazakii* with MIC values ranging from 50 to 100 μg mL^{-1}. Compound **3g** showed highest antibacterial activity against E. *coli* (MIC = 50 μg mL^{-1}). In silico drug-likeness, pharmacokinetic (ADME) properties, toxicity effects, and drug scores were also evaluated, and none of the sixteen compounds were found to violate Lipiniski's rule of five or Veber's rule, indicating potential for development as oral drug candidates. In addition, a docking study of compound **3i** into the active site of *E. coli* FabH receptor, an attractive target for the development of new antibacterial agents, showed it has good binding properties.

Keywords 4-Arylthiazoles · ADME properties · Antibacterial activity · Cytotoxicity · Docking study · Drug-likeness

Introduction

Molecules possessing the small and ostensibly simple 1,3-thiazole heterocyclic substructure often have surprisingly complex biological properties. Thiazoles and their derivatives are an important class of five-member heterocyclic compounds, and contain sulfur and nitrogen at positions 1 and 3 of the thiazole ring, respectively. The thiazole scaffold is found in a variety of natural bioactive compounds used as pharmaceuticals and agrochemicals. Thiazole analogues have continued to attract interest in medicinal chemistry field during the past decades due to their wide ranging biological activities, which include antibacterial (Alam et al. 2011), antifungal (Sarojini et al. 2010), antiviral (El-Sabbagh et al. 2009), anti-inflammatory (Helal et al. 2013), anticancer (Soares et al. 2013), antioxidant (Shih and Ying 2004), antitubercular (Romagnoli et al. 2011), antiplasmodial (Mjambili et al. 2014), antiallergic (Ban et al. 1998), anti-inflammatory (Deb et al. 2014), antipsychotropic (Zablotskaya et al. 2013), antiarthritic (Nishikaku and Koga 1993), neuroprotective (Zhang et al. 2009), and antidiabetic (Iino et al. 2009) effects. Moreover, the 1,3-thiazole scaffold is commonly utilized in drug development, and found in many commercially available drugs, including tenonitrozole (an antiparasitic) (Cohen et al. 2012), penicillin derivatives (antibacterial) (Ye et al. 2013), vitamin B1 (thiamine) (Wei

Electronic supplementary material The online version of this article (doi:10.1007/s13765-016-0148-9) contains supplementary material, which is available to authorized users.

✉ Dong-Ung Lee
dulee@dongguk.ac.kr

[1] Division of Bioscience, Dongguk University, Gyeongju 780-714, Republic of Korea

[2] Department of Chemistry, Jagannath University, Dhaka 1100, Bangladesh

et al. 2014), bleomycin (anticancer) (Rahmutulla et al. 2014), tiazofurin (antineoplastic) (Popsavin et al. 2006), ritonavir (anti-HIV) (Sevrioukova and Poulos 2013), fanetizole (Styrt et al. 1985), meloxicam (anti-inflammatory) (Novakova et al. 2014), and nizatidine (antiulcer) (Jain et al. 2015). Recently, it was reported that some new triazolyl-thiazole, 2-thiazolylhydrazone, and phenylthiazole analogues showed anti-Alzheimer's disease activity (Shiradkar et al. 2007), monoamine oxidase (MAO) inhibitory activity (Chimenti et al. 2007), and selective acetyl-Co-A carboxylase inhibitory activity (Clark et al. 2007), respectively. More recently, Netalkar et al. (2014) reported some novel benzothiazole/transition metal complexes exhibit DNA binding and cleavage properties and anti-tuberculosis activity, and Turan-Zitouni et al. (2011) described some new (3,4-diaryl-3H-thiazol-2-ylidene)pyrimidin-2-yl amine derivatives with anti-HIV activity.

Due to the emergence of bacterial resistance to almost all commercial antibiotics, the treatment of infectious disease has become a challenging problem in hospitals and communities, and thus, the identification of new antibacterial agents with novel targets is of considerable importance. In particular, fatty acid biosynthesis (FAB) is a promising target for new antibacterial agents (Price et al. 2001), because it is essentially required for bacterial cell viability and growth. β-Ketoacyl-acyl carrier protein (ACP) synthase III, which is also known as FabH or KAS III, plays an important role in bacterial FAB (Khandekar et al. 2003), and thus, bacterial FabH is an attractive target for the design of new antibiotics. A literature survey revealed some thiazoles that potently inhibit FabH possess an amide (–NHCO–) or azomethine amine (–C=N–NH–) moiety at the 2-position of the thiazole ring exhibit antibacterial activity (Lv et al. 2009; Sarojini et al. 2010; Lee et al. 2012; Yang et al. 2012; Li et al. 2014). Furthermore, these structural motifs are also present in many pharmaceutically active compounds. Figure 1 shows structures of several reported antibacterial FabH inhibitors that possess a thiazole scaffold. In our previous study, we reported the synthesis and antimicrobial and antioxidant activities of a series of 2-arylidenehydrazinyl-4-arylthiazole analogues (Alam et al. 2014a). In the present study, we describe the in vivo cytotoxic activities and minimum inhibitory concentration (MIC) values of sixteen 2-arylidenehydrazinyl-4-arylthiazole analogues (**3a**–**p**) against two Gram-positive *(Listeria monocytogenes* and *Enterococcus faecalis*) and two Gram-negative bacterial strains (*Cronobacter sakazakii* and *E. coli*). The synthesis of compounds **3a**–**p** have been demonstrated in our previous study (Alam et al. 2014a); however, in vivo cytotoxic actions and MIC values of compounds **3a**–**p**, have not yet been reported. In addition, an in silico study was performed to predict the drug-likeness, pharmacokinetic properties, e.g., absorption, distribution, metabolism, and elimination (ADME), MTIR (mutagenic, tumorigenic, irritant, and reproductive) toxicity profiles, and drug scores in an effort to identify molecular features responsible for the cytotoxic properties of these compounds. Furthermore, docking simulations were performed using the X-ray crystallography determined structure of *E. coli* FabH to investigate binding modes at its active site. Molecular docking is a computer-assisted drug design method that is usually used to predict the favorable binding conformations of ligands at active sites of target receptors. It also provides information regarding the natures of bonding interactions, which contribute to binding affinities between ligands and receptors

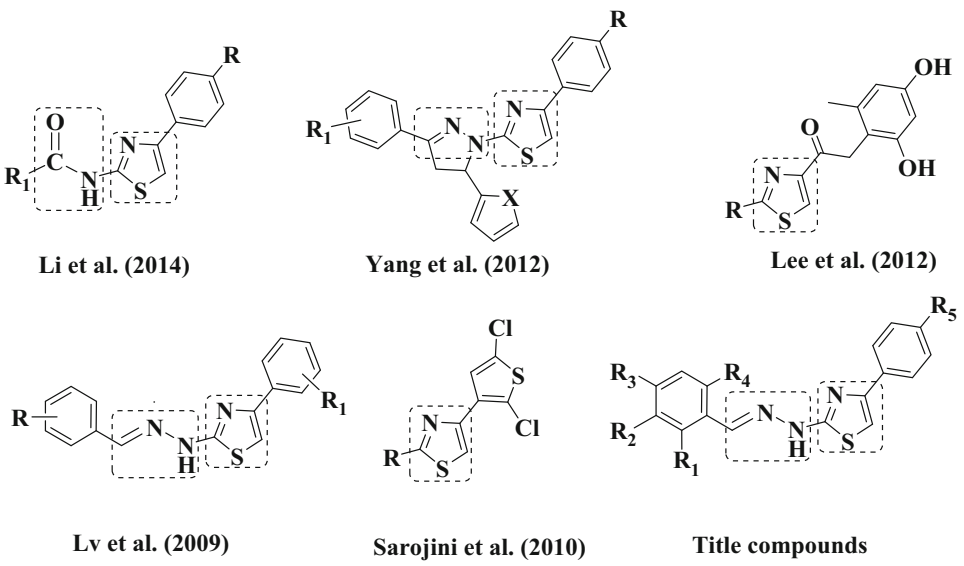

Fig. 1 The structures of several reported antibacterial FabH inhibitors with pharmacodynamic scaffolds similar to the 2-arylidenehydrazinyl-4-arylthiazole analogues

(Sarojini et al. 2010). Therefore, molecular docking is considered an important in silico tool for pharmaceutical lead discovery (Shoichet et al. 2002).

Materials and methods

Synthesis

The 2-arylidenehydrazinyl-4-arylthiazole analogues (**3a–p**) used in the present study were prepared as we previously described (Alam et al. 2014a) from their corresponding arylidenethiosemicarbazones (**2a–j**) as presented in Scheme 1. Briefly, to a stirred solution of thiosemicarbazide (1 mmol) in an ethanol–water mixture (1:1), an ethanolic solution of a substituted benzaldehyde (1 mmol) was added slowly and refluxed for 10–20 min. After cooling the reaction mixture to ambient temperature, the mixtures obtained were filtered to provide solid crude products, which were crystallized from ethanol to furnish pure compounds **2a–j** at yields of 83–94 %. The arylidenethiosemicarbazones (1 mmol) so obtained were refluxed with 2-bromoacetophenone or 2,4′-dibromoacetophenone (1 mmol) in ethanol for 30–60 min and then cooled to ambient temperature. The resulting precipitates were filtered and washed with water to give crude products, which were purified by crystallization from DMF-EtOH (1:1) to afford the pure 1,3-thiazole derivatives (**3a–p**) at yields of 72–95 %.

Cytotoxicity assay

Brine shrimp nauplii (*A. salina*) were used for the in vivo cytotoxicity assay, which was performed as described by Mayer et al. (1982), with some modifications. Briefly, brine shrimp nauplii were hatched in a small tank containing artificial seawater (3.8 % NaCl). The tank was partially exposed to incandescent light to attract the nauplii. The assay was performed 24 h after hatching; no food was provided during hatching or the experimental periods. Test samples (3 mg) were dissolved in 0.6 mL of DMSO to obtain stock solutions of 5 mg mL^{-1}. Different concentrations of test samples (5 mL made up artificial seawater) were then placed in separate vials. Twenty brine shrimp nauplii were then placed in each vial. The negative control was prepared in the same manner, except the sample was omitted. Gallic acid was used as the positive control. After for incubation 24 h, the vials were observed using a magnifying glass and the numbers of survivors were counted. Tests were performed in triplicate, and LC_{50} values in ppm were obtained from resulting data using Probit analysis software (Finney 1978).

Antibacterial screening

MIC (μg mL^{-1}) of compounds (**3a–p**) were determined against *Listeria monocytogenes* ATCC 43256 (G^+), *Enterococcus faecalis* CARS 2011-012 (G^+), *Cronobacter sakazakii* CARS 2012-J-F (G^-), and *E. coli* CARS 2011-016 (G^-) using nutrient broth medium (DIFCO) and a serial dilution technique (Nishina et al. 1987). MIC was defined as the lowest concentration of the tested compound (in DMSO) that inhibited bacterial growth.

Determination of drug-likeness and ADME properties

The Molinspiration property toolkit (Molinspiration Cheminformatics, Bratislava, Slovak Republic) was used to determine the drug-likeness properties of the synthesized compounds, that is, molecular polar surface area (TPSA), octanol–water partition coefficient (logP), number of rotatable bonds (NROTB), molecular volume, number of hydrogen donors (HBD), and number of hydrogen acceptors (HBA). Toxicities (mutagenic, tumorigenic, irritant, and reproductive), drug scores, and solubility parameters were calculated using Osiris program (Osiris Property Explorer ver. 2, Allschwil, Switzerland). Absorption percentages were calculated using the formula: % ABS = 109 − (0.345 × TPSA).

Docking studies

The molecular geometries of compounds **3c**, **3i**, and **3j** were investigated using standard bond lengths and angles

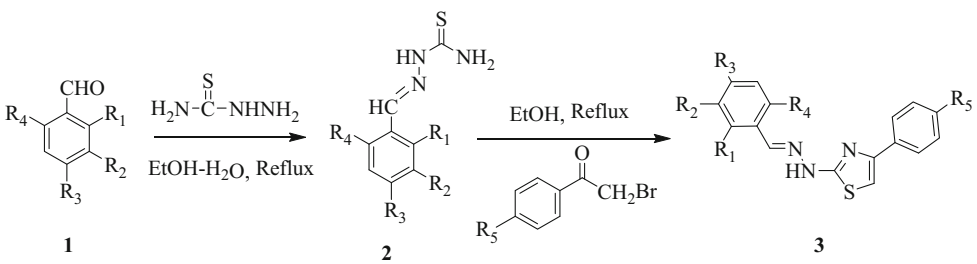

Scheme 1 Syntheses of 2-arylidenehydrazinyl-4-arylthiazole analogues **3a–p**

using the ChemBio3D Ultra 14.0 molecular modeling program (CambridgeSoft Corporation, Cambridge, MA 02140 USA). The molecular energies were minimized using a semi-empirical molecular orbital AM1 method (Dewar et al. 1985) using GAMESS Interface in the ChemBio3D Ultra Ver. 14.0. The crystal structure of *E. coli* FabH-CoA complex was obtained from Protein Data Bank (PDB code: 1HNJ) for docking studies. All bound water and co-crystallized ligand were eliminated and polar hydrogen atoms and Kollman-united charges were added to molecules. The pdb and pdbqt files of ligands and the receptor were prepared using AutoDock 4.2 software. Free rotation was allowed about single bonds during docking. Docking was conducted using the standard protocol implemented by AutoDock Vina in PyRx 0.8 software and the geometries of resulting complexes were investigated using Discovery Studio 4.0 (Accelrys, Inc. San Diego, CA 92121 USA) and Molegro Molecular viewer 2.5 (CLC bio company, Waltham, MA 02451 USA).

Molecular descriptors and field points

Calculations of geometrical descriptors and field point maps of compounds **3c**, **3i**, and **3j** were performed to investigate molecular surface properties using ChemAxon (ChemAxon LLC, Cambridge, MA 02142 USA) and TorchLite software (Cresset BioMolecular Discovery Ltd., Cambridgeshire, SG8 0SS, UK). Representative field points are presented using colors and sizes, and larger field points indicate stronger potential interactions.

Results and discussion

Cytotoxic activities

The in vivo cytotoxic activities of compounds (**3a**–**p**) were screened using an *Artemia salina* (brine shrimp) lethality bioassay as previously described (Alam et al. 2014a, b). This bioassay is an excellent tool for the preliminary screening of bioactive compounds (Mayer et al. 1982; Hartl and Humpf 2000). Lethal doses (LC_{50}) obtained using the brine shrimp assay can be used to determine more specific activities (Weidenbörner and Chandra Jha 1993; Alam et al. 2014a). The results obtained for 2-arylidenehydrazinyl-4-arylthiazole analogues (**3a**–**p**) are presented in Table 1. Gallic acid was also tested under identical conditions as a positive control. Of the tested compounds, **3g** showed greatest brine shrimp toxicity with a LC_{50} of 54 ppm, followed by compounds **3h** (LC_{50} = 85 ppm) and **3e** (LC_{50} = 113 ppm). However, all compounds were less cytotoxic than gallic acid (LC_{50} = 12 ppm). Compounds **3f, 3k**, and **3l** showed moderate cytotoxicity with LC_{50} values of 319, 522, and 848 ppm, respectively, whereas compounds **3a** and **3p** exhibited low activities with LC_{50} values of 1933 and 1794 ppm, respectively. On the other hand, compounds **3b**–**3d**, **3m,** and **3n** demonstrated similar weak activities ($LC_{50} > 2500$ ppm) and compounds **3i**, **3j**, and **3o** were not cytotoxic to *A. salina*.

In most compounds, the substituent types and positions play significant role to exert cytotoxic activity. Structure–activity relationships (SAR) may be explained briefly as follows: introduction of a moderate electron donating group (OMe) at the R_1 and R_3 or R_2 and R_3 positions favored activity (e.g., **3 g** or **3e**), while the presence of a more polar group (OH) at the same positions caused reduced activity (e.g., **3a** and **3c**). Substitution of a bromine atom (a bulky and moderate ring deactivating group) at R_5 position greatly decreased cytotoxicity (e.g., **3 g** > **3 h** or **3e** > **3f**).

Antibacterial activities

The MICs (minimum inhibitory concentrations) of compounds **3a**–**p** were evaluated using two gram-positive bacterial strains, *L. monocytogenes* ATCC 43256 and *E. faecalis* CARS 2011-012, and two gram-negative bacterial strains, *C. sakazakii* CARS 2012-J-F and *E. coli* CARS 2011-016 using the serial dilution method. MIC values are presented in Table 2. The antibacterial nalidixic acid was used as a positive control. All synthesized compounds showed antibacterial activity and MIC values ranged from 50 to 300 μg mL^{-1}. Compounds **3c**, **3g**, **3i**, **3j**, and **3m** exhibited significant antibacterial activity. Summarizing, compounds **3c**, **3i**, and **3j** had lowest MIC values (~50 μg mL^{-1}) against *L. monocytogenes*, whereas **3i** and **3 m** had similar MIC values (50 μg mL^{-1}) against *E. faecalis*. Compounds **3b**, **3c,** and **3i** had the lowest MIC values (~100 μg mL^{-1}) against *C. sakazakii*, and compound **3 g** had the lowest MIC value (50 μg mL^{-1}) against *E. coli*. However, nalidixic acid had the strongest effect with MIC values ranging from 12.5 to 25 μg mL^{-1}.

The results presented in Table 2 indicate that structure–antimicrobial activity relationships did not appear to play a significant role as all compounds exhibited similar MIC values ranging from 100 to 200 μg mL^{-1} against all bacterial strains with some exceptions of compounds **3c**, **3g**, **3i**, **3j**, and **3 m** against some selected bacterial strains (MIC = 50 μg mL^{-1}). This result led us to speculate that the mode of action of these compounds is microorganism dependent. However, the presence of an electron donating group (OH or OMe) at the *ortho*- and *para*-positions favored activity, e.g., **3c** and **3i** against *L. monocytogenes*, **3g** against *E. coli*, **3i** and **3m** against *E. faecalis*, while the presence of these groups at the *meta*-position greatly reduced activity (e.g., **3a** and **3k**). Introduction of a

Table 1 Cytotoxicities of the 2-arylidenehydrazinyl-4-arylthiazole analogues (**3a–p**) and of gallic acid (positive standard)

Comp.	Substituents					Mortality, LC_{50} (ppm)	Regression equation[c]	R^{2d}
	R_1	R_2	R_3	R_4	R_5			
3a	H	OH	OH	H	H	1933 (1582–2640)[a]	$Y = 1.706X - 0.6058$	0.97
3b	H	OH	OH	H	Br	>2500 (10[b])	–	–
3c	OH	H	OH	H	H	>2500 (20[b])	–	–
3d	OH	H	OH	H	Br	>2500 (10[b])	–	–
3e	H	OCH_3	OCH_3	H	H	113 (93–151)[a]	$Y = 1.8133X + 1.281$	0.95
3f	H	OCH_3	OCH_3	H	Br	319 (255–434)[a]	$Y = 1.4667X + 1.325$	0.96
3g	OCH_3	H	OCH_3	H	H	54 (46–65)[a]	$Y = 2.2933X + 1.145$	0.98
3h	OCH_3	H	OCH_3	H	Br	85 (73–101)[a]	$Y = 2.12X + 0.9065$	0.9898
3i	OH	H	OH	OH	H	NA	–	–
3j	OH	H	OH	OH	Br	NA	–	–
3k	H	OCH_3	OH	H	H	522 (447–624)[a]	$Y = 1.9877X - 0.391$	0.95
3l	H	OCH_3	OH	H	Br	848 (733–1008)[a]	$Y = 2.12X - 1.2135$	0.98
3m	H	H	OH	H	Br	>2500 (15[b])	–	–
3n	OH	H	H	H	Br	>2500 (10[b])	–	–
3o	H	H	Cl	H	Br	NA	–	–
3p	H	H	$N(CH_3)_2$	H	Br	1794 (1538–2214)[a]	$Y = 2.096X - 1.8228$	0.94
Gallic acid						12 (9–16)[a]	$y = 1.1733x + 3.7193$	0.97

[a] 95 % confidence limits

[b] Mortality percentage at 25,000 ppm

[c] Obtained from Log (conc.) versus probit correlation

[d] Log (conc.) versus probit correlation coefficient

NA not active

Table 2 In vitro minimum inhibitory concentration (MIC) profiles of 2-arylidenehydrazinyl-4-arylthiazole analogues **3a–p**

Comp.	Substituents					MIC (μg mL^{-1})			
	R_1	R_2	R_3	R_4	R_5	Gram-positive		Gram-negative	
						L. m.	*E. f.*	*C. s.*	*E. c.*
3a	H	OH	OH	H	H	150	200	150	200
3b	H	OH	OH	H	Br	150	200	100	200
3c	OH	H	OH	H	H	50	NA	100	200
3d	OH	H	OH	H	Br	200	NA	200	300
3e	H	OCH_3	OCH_3	H	H	150	100	150	200
3f	H	OCH_3	OCH_3	H	Br	100	150	150	150
3g	OCH_3	H	OCH_3	H	H	200	NA	200	50
3h	OCH_3	H	OCH_3	H	Br	100	200	200	150
3i	OH	H	OH	OH	H	50	50	100	150
3j	OH	H	OH	OH	Br	50	150	200	200
3k	H	OCH_3	OH	H	H	200	NA	200	300
3l	H	OCH_3	OH	H	Br	150	200	200	200
3m	H	H	OH	H	Br	100	50	150	200
3n	OH	H	H	H	Br	150	100	200	200
3o	H	H	Cl	H	Br	200	NA	200	300
3p	H	H	$N(CH_3)_2$	H	Br	200	NA	200	300
Nalidixic acid						25	25	12.5	12.5

L. m Listeria monocytogenes ATCC 43256; *E. f. Enterococcus faecalis* CARS 2011-012*; C. s. Cronobacter sakazakii* CARS 2012-J-F; *E. c. E. coli* CARS 2011-016; *NA* not active

Table 3 Calculated using Lipinski's rule of five, Veber's rule, and solubility and the absorption parameters of the 2-arylidenehydrazinyl-4-arylthiazole analogues (**3a–p**) and doxorubicin (positive standard)

Comp.	Lipinski's violations (≤1)	Based on Lipinski rule				Based on Veber rule		logS[g]	%ABS[h]
		HBA[a] (≤10)	HBD[b] (≤5)	clogP[c] (≤5)	MW[d] (≤500)	NROTB[e] (≤10)	TPSA[f] (≤140 Å^2)		
3a	0	5	3	3.198	311.36	4	77.739	−4.07	82.18
3b	0	5	3	3.508	390.26	4	77.739	−4.90	82.18
3c	0	5	3	3.394	311.36	4	77.739	−4.07	82.18
3d	0	5	3	4.203	390.26	4	77.739	−4.90	82.18
3e	0	5	1	3.504	339.42	6	55.751	−4.70	89.77
3f	0	5	1	4.213	418.31	6	55.751	−5.53	89.77
3g	0	5	1	3.999	339.42	6	55.751	−4.70	89.77
3h	0	5	1	4.508	418.31	6	55.751	−5.53	89.77
3i	0	6	4	3.511	327.36	4	97.967	−3.77	75.20
3j	0	6	4	4.355	406.26	4	97.967	−4.61	75.20
3k	0	5	2	3.296	325.39	5	66.745	−4.38	85.97
3l	0	5	2	4.105	404.28	5	66.745	−5.22	85.97
3m	0	4	2	4.187	374.26	4	57.511	−5.20	89.16
3n	0	4	2	4.857	374.26	4	57.511	−5.20	89.16
3o	0	3	1	5.444	392.70	4	37.283	−6.23	96.14
3p	0	4	1	4.868	401.33	5	40.521	−5.53	95.02
Nalidixic acid	0	5	1	0.54	232.24	2	70.5	−2.67	84.68
Gallic acid	0	5	4	0.11	170.12	1	97.99	−0.74	75.19

[a] Number of hydrogen bond acceptors

[b] Number of hydrogen bond donors

[c] Calculated octanol/water partition coefficient

[d] Molecular weight

[f] Molecular polar surface area

[e] Number of rotatable bonds

[f] Topological polar surface area

[g] Solubility parameter

[h] Percentage absorption

bromine atom (a bulky as well as moderate ring deactivating group) at R_5 position greatly reduced antibacterial efficacy (e.g., **3i** > **3j** or **3c** > **3d**), which would be due to the size effect or steric effect.

Pharmacokinetic and drug-likeness properties

Absorption, distribution, metabolism, and elimination (ADME) are crucial potential drug parameters. To assess drug-likeness of a compound, Lipiniski's rule of five (ROF) and Veber's rule are usually used. These rules consider the following parameters: topological polar surface area (TPSA), octanol–water partition coefficient (logP), NROTB, HBD and acceptors (HBA), and molecular weight (MW). logP and PSA have been shown to be excellent descriptors of drug absorption (including intestinal absorption), bioavailability, Caco-2 permeability, and blood–brain barrier penetration. Therefore, we studied the synthesized compounds (**3a–p**) in silico to assess ADME and drug-likeness properties and then compared these with nalidixic acid and gallic acid controls. The descriptors of Lipinski's ROF and Veber's rule (TPSA, logP, NROTB, HBD, HBA, and MW) were calculated using the Molinspiration online property toolkit (Lipinski et al. 2001), and results obtained are presented in Table 3. TPSA was calculated using the method developed by Ertl et al. (2000), which considers the sum of fragment contributions, and O- and N- centered polar fragments. The results obtained showed that none of the sixteen synthesized compounds violated Lipiniski's or Veber's rule, suggesting good drug-like properties. The four major developmental criteria of an orally active drug candidate are logP ≤ 5, MW ≤ 500, HBA ≤ 10, and HBD ≤ 5 (Ertl et al. 2000). The calculated logP and logS values of the of the synthesized compounds were within the ranges of 3.198 to 5.44 and −4.07 to −6.23, respectively; these values are −2.0 to 6.5 and 0.5

Comp.	Toxicity effects			
	M	T	I	R
3a	Low	High	Low	Low
3b	Low	High	Low	Low
3c	Low	High	Low	Low
3d	Low	High	Low	Low
3e	Low	High	Low	Low
3f	Low	High	Low	Low
3g	Low	High	Low	Low
3h	Low	High	Low	Low
3i	Low	High	Low	Low
3j	Low	High	Low	Low
3k	Low	High	Low	Low
3l	Low	High	Low	Low
3m	Low	High	Low	Low
3n	Low	High	Low	Low
3o	Low	High	Low	Low
3p	Low	High	Low	Low
Nalidixic Acid	High	High	Low	High
Gallic Acid	High	Low	Low	High

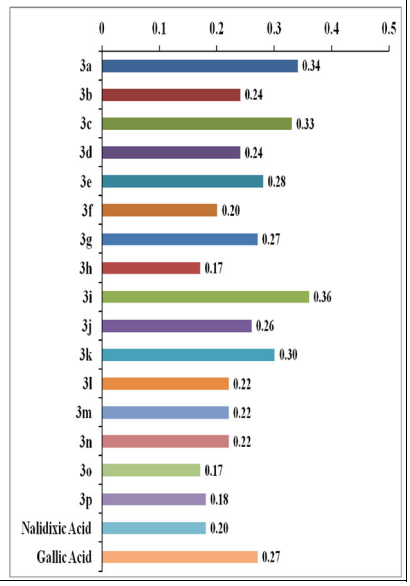

Fig. 2 Toxicity profiles (*left*) and drug scores (*right*) of the sixteen 2-arylidenehydrazinyl-4-arylthiazole analogues (**3a–p**) and of the standard antibacterial and cytotoxic agents, nalidixic acid and gallic acid (*M* mutagenic; *T* tumorigenic, *I* irritant; *R* reproductive)

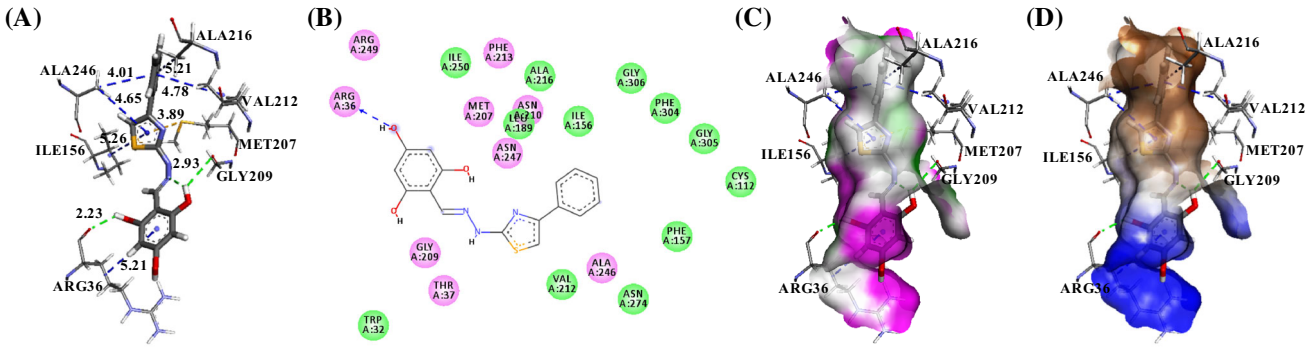

Fig. 3 **(A)** Binding model of compound **3i** with *E. coli* FabH (Protein Data Bank entry: 1HNJ). The *green dotted lines* show hydrogen bonds, the *blue dotted lines* show π–alkyl interactions, and the *yellow dotted lines* show π–sulfur interactions. (**B**) 2D ligand interaction diagram with *E. coli* FabH obtained using the Discovery Studio program; essential amino acid residues at the binding site are tagged in *circles*. The *purple circles* show amino acids that participate in electrostatic and covalent interactions and the *green circles* show amino acids involved in van der Waals' interactions. (**C**) Hydrogen bond interactions shown as donor (*pink*) and acceptor surfaces (*green*). (**D**) Hydrophobic interactions (*brown*)

to −6.5, respectively, for 95 % of commercial drugs (Deb et al. 2014). Noticeably, all synthesized compounds exhibited excellent absorption % values (75.20–96.14). According to predicted human oral absorption, 80 and 25 % indicate excellent and poor drug absorption, respectively. However, some FDA-approved drugs fail to satisfy Lipiniski's ROF, and it has been reported that 30 % of drugs violate this rule (Zhang and Wilkinson 2007).

Cytochrome P450 is an important enzyme and is responsible for many ADME problems. Its inhibition or the generation of redundant metabolites by cytochrome P450 can result in many adverse drug side effects. The prediction of ADME-toxicity is important prior to structural drug design and many potential drugs fail to reach the clinical stage because of ADME-Tox issues. Hence, we examined the mutagenicities, tumorigenicities, irritancies, and reproductive toxicities and drug scores (Sadowski and Kubinyi 1998) of the sixteen synthesized compounds and compared them with those of the nalidixic and gallic acid standards using the Osiris program. Results are presented in Fig. 2. Osiris predicted that none of the sixteen compounds would have irritant, mutagenic, or reproductive toxicity, but all were predicted to have high tumorigenic toxicity. Interestingly, nalidixic acid was predicted to have high mutagenic, tumorigenic, and reproductive effects, whereas gallic acid was predicted to have high mutagenic and reproductive effects. Most of the sixteen compounds (except compounds **3h**, **3o**, and **3p**) had a higher drug

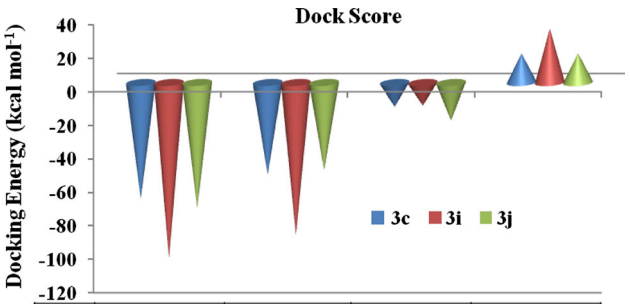

Comp.	Total Energy	vdW	H-bond	AverConPair
3c	-69.443	-54.8878	-14.5552	17.3182
3i	-104.908	-91.1249	-13.7835	32.375
3j	-75.0625	-52.3552	-22.7073	17.5833

Fig. 4 Predicted docking energies of compounds **3c**, **3i,** and **3j** based on docked poses into the active site of *E. coli* FabH

scores than nalidixic acid, whereas only compounds **3a, 3c,** and **3i** had a higher drug score than gallic acid. The above in silico ADME results suggest 2-arylidenehydrazinyl-4-arylthiazole analogues (**3a**–**p**) have good drug-likeness properties and that they represent pharmacologically active base worthy of further study.

Molecular docking studies

In order to predict whether the 2-arylidenehydrazinyl-4-arylthiazole analogues could bind to the FabH receptor to exert their antibacterial activity, the most active (**3c**, **3i**, and **3j)** compounds were docked into the active site of *E. coli* FabH (PDB ID: 1HNJ) using AutoDock tools 1.5.6 (Morris et al. 2009) and AutoDock Vina in PyRx 0.8 software (Trott and Olson 2010). *E. coli* β-ketoacyl-(acyl carrier protein) synthase III, also known as ecKAS III or FabH, plays an essential, regulatory role in the bacterial fatty acid synthesis. The enzyme initiates fatty acid elongation cycles and is involved in the feedback regulation of the biosynthetic pathway (Heath and Rock 1996). Furthermore, the FabH proteins of Gram-positive and Gram-negative bacteria are highly conserved at the sequence and structural level (there are no significant homologous proteins in man). In addition, the residues that comprise the active site are essentially invariant among Gram-positive and Gram-negative organisms (Nie et al. 2005). Therefore, FabH represents a promising target for the design of novel, selective, nontoxic, broad-spectrum antimicrobial drugs. The crystal structure of *E. coli* FabH-CoA complex was retrieved from the Protein Data Bank (PDB ID: 1HNJ) and molecular docking of compounds **3c**, **3i**, and **3j** were performed at its active site. The results obtained showed that compounds **3c**, **3i**, and **3j** bind to the same active site of FabH receptor as the endogenous ligand (malonyl CoA) and other reported thiazole FabH inhibitors (Lv et al. 2009; Cheng et al. 2013; Li et al. 2014). The binding model and the different types of interactions found for the most active compound **3i** are shown in Fig. 3, and the docking models for compounds **3c** and **3j** are provided as supporting data (Supplementary Figs. 1, 2, respectively). Since docking scores provide a measure of ligand to receptor binding affinity, we calculated binding scores for compounds **3c**, **3i**, and **3j** using iGEMDOCK software (Yang and Chen 2004) (results are presented in Fig. 4). The binding affinities of compounds **3c**, **3i,** and **3j** with FabH receptor were found to be −69.443, −104.908, and −75.0625 kcal mol^{-1} with van der Waals contributions of −54.8878, −91.1249, and −52.3552 kcal mol^{-1}, respectively, and H-bond contributions of −14.5552, −13.7835, and −22.7073 kcal mol^{-1},

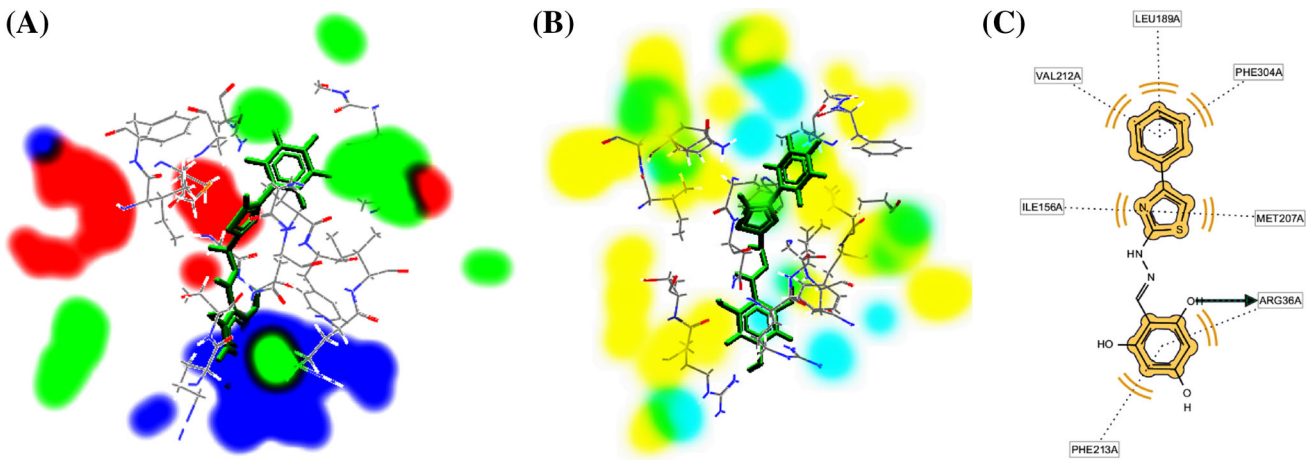

Fig. 5 Energy map of compound **3i** at the *E. coli* FabH binding site. (**A**) The *green, red,* and *blue* regions are energetically favorable for steric and negative- and positive-electrostatic interactions, respectively. (**B**) The *yellow* and *cyan* regions are energetically favorable for H-bond donor and acceptor interactions, respectively. (**C**) Pharmacophore model of protein–ligand interactions

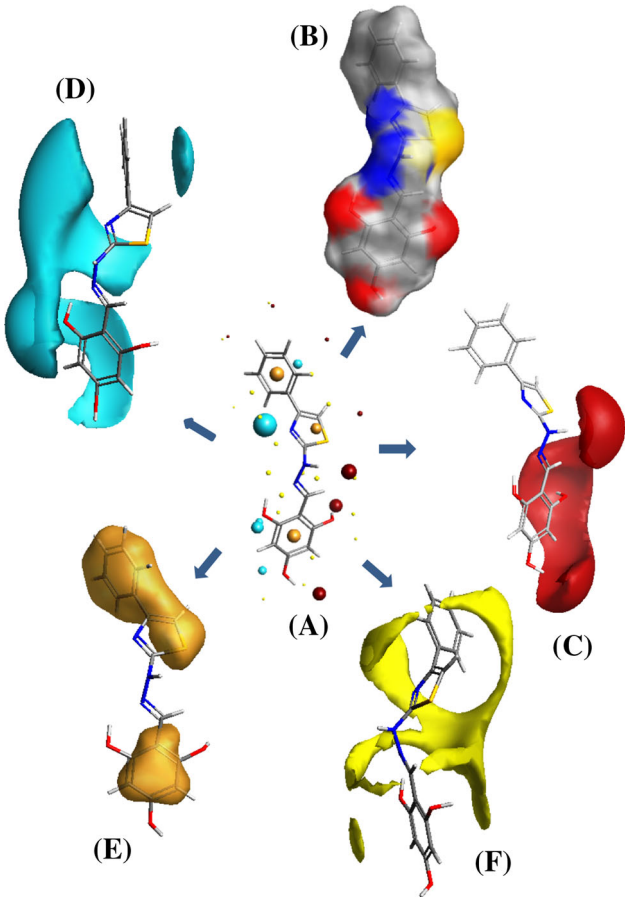

Fig. 6 Field patterns and physicochemical properties of compound **3i**. (**A**) The *cyan*, *red*, *yellow*, and *gold* points indicate negative, positive, surface, and hydrophobic fields, respectively, potentially involved in ligand/receptor interactions. (**B**) *White smoky regions* indicate solvent-accessible surfaces. (**C**) Positive field (*red*) points are predicted to interact with negatives/H-bond acceptors on a receptor. (**D**) Negative field (*cyan*) points are predicted to interact with positives/H-bond donors on a receptor. (**E**) van der Waals surface field (*yellow*) points are involved in vdW interactions. (**F**) Hydrophobic field (*gold*) points indicate regions of high polarizability/hydrophobicity

respectively. These results indicate that compound **3i** binds more tightly to the active site of FabH receptor than compounds **3c** or **3j** due to its greater van der Waals', hydrophobic, and hydrogen bonding interactions. In the binding model of **3i** and *E. coli* FabH receptor, the carbonyl group of ARG36 (O…H–O: 2.23 Å) and the GLY209 (O…H–O: 2.93 Å) amino acid residues form hydrogen bonds with the *ortho*-hydroxyl groups of the benzylidene phenyl ring. However, in the binding model of **3c** with *E. coli* FabH receptor, the carbonyl group of GLY152 (O…H–O: 2.40 Å) amino acid residue form hydrogen bond, whereas for **3j** and *E. coli* FabH receptor, the carbonyl group of GLY209 (O…H–O: 2.03 Å) and the amino hydrogen of the ASN247 (N–H …O: 2.21 Å) amino acid residues form hydrogen bonds with the *ortho*-hydroxyl groups of the benzylidene phenyl ring. In addition to hydrogen bonding interactions, compounds **3c** and **3i** exhibited π–sulfur interactions with MET207 (4.10 and 3.89 Å, respectively) amino acid residues, and **3c** also showed π–pi interactions with the TRP32 (5.17 Å) amino acid residue. In addition, π–alkyl interactions with ILE156 (5.38), VAL212 (4.68), and ALA246 (3.98) for **3c**, ARG36 (5.21), ILE156 (5.26), VAL212 (4.78), ALA216 (5.21), and ALA246 (4.01 and 4.65) for **3i**, and ARG151 (8.82), ILE156 (5.49), MET207 (5.09), and ALA246 (4.26) for **3j** were found to involve thiazole, phenyl-, or benzylidene-phenyl rings. The following van der Waals' interactions were also observed: between **3c** and TRP32, CYS112, ILE250, ASN210, PHE213, ASN274, PHE157, LEU189, PHE304, and GLY305; between **3i** and TRP32, CYS112, PHE157, LEU189, ILE250, ASN274, PHE304, GLY305, and GLY306; and between **3j** and TRP32, THR37, GLY152, PHE157, LEU189, ILE250, VAL212, and HIS244. The above results indicate compounds **3c**, **3i,** and **3j** bind to the same active site of FabH receptor and suggest that the higher binding affinity of **3i** might is caused by strong van der Waals' interactions with amino acid residues at the active site of FabH.

The energy maps of receptor ligand binding sites are useful for understanding the different types of molecular interactions in favorable regions. Molecular docking studies are also used to identify pharmacophore, that is, common chemical frameworks responsible for a drug's biological activity. Therefore, the energy maps and pharmacophore models of compounds **3c**, **3i**, and **3j** were also studied at the FabH receptor binding site using Molegro Molecular viewer 2.5 and LigandScout 3.12 software, respectively. Energy maps and the pharmacophore model of compound **3i** are shown in Fig. 5, and energy maps for compounds **3c** and **3j** are provided as supporting data (Supplementary Figs. 3, 4, respectively). Referring to Fig. 5A, green regions are energetically favorable for steric interactions, whereas red and blue color regions are energetically favorable for negative- and positive-electrostatic interactions, respectively, in the **3i**-FabH receptor complex. Yellow and cyan indicate regions where H-bond donor and acceptor interactions are energetically favorable, respectively, at the **3i** binding site in FabH receptor (Fig. 5B). Because compounds **3c**, **3i**, and **3j** bind to the same site, their pharmacophore models were similar (c.f. Supplementary Figs. 3C, 4C, 5C, respectively).

Field points and molecular descriptors

Field points consist of electrostatic, van der Waals, and hydrophobic potentials and molecular descriptors, for example, quantum-chemical, grid-based, volume, and surface descriptors, of a molecule that play significant roles in

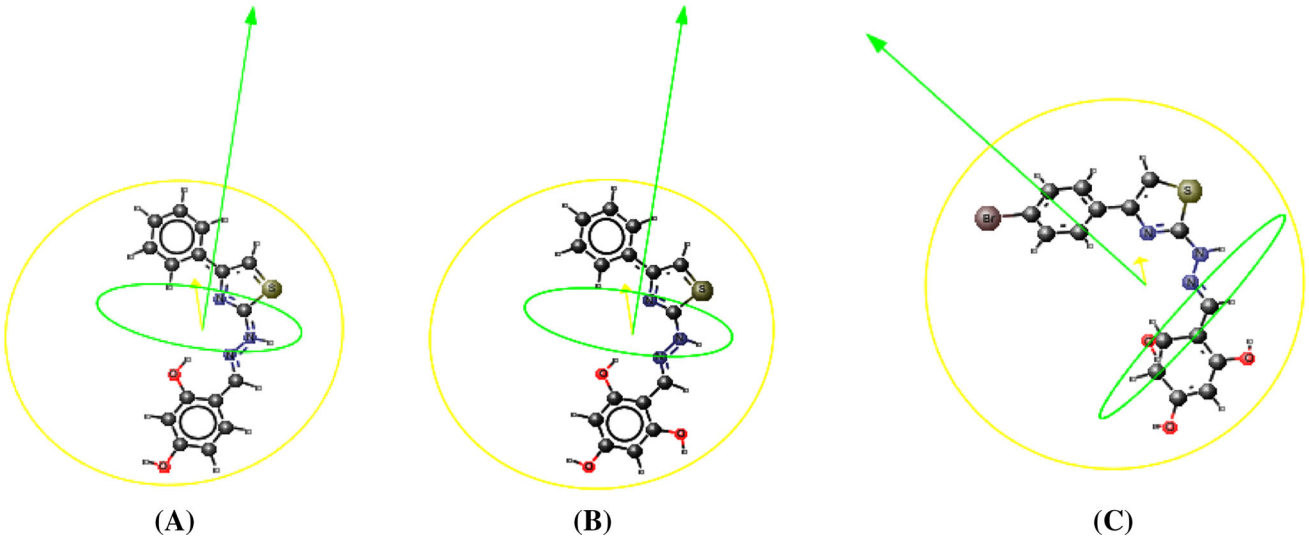

Fig. 7 Geometrical structures of compounds **3c** (**A**), **3i** (**B**), and **3j** (**C**) showing van der Waals volumes and lengths of maximum (*yellow*) and minimum (*green*) areas perpendicular to each other

its chemical and biological activities. The field points of a molecule provide more information on pharmacophore and enable the position and potentials of electrostatic, van der Waals, and hydrophobic interaction points to be directly measured from the physical properties of a molecule. Molecular field patterns, that is, the electrostatic (positive and negative), steric, and hydrophobic properties, of compound **3i** are presented in Fig. 6, and those of compounds **3c** and **3j** are provided as supporting data (Supplementary Figs. 5, 6, respectively). These field point patterns are used to express ligand–receptor interactions simultaneously. The nature of bonding and the abilities of ligands to interact with receptors are categorized using the sizes of field points and larger field points are indicative of strong potential interactions. In addition, geometrical 3D descriptors of the surface interactions of compounds **3c**, **3i,** and **3j** were also analyzed and are presented in Fig. 7 showing their three-dimensional representation in relation to the nature and connectivity of the atoms as well as the overall spatial configurations. The geometrical 3D descriptors are usually use to effective search for the relationships between the molecular structure and biological activities of a molecule. The geometrical 3D descriptors of compounds **3c**, **3i**, and **3j** are as follows: the dreiding energy, which is the energy related to the 3D structure of the molecule using the dreiding force field (Mayo et al. 1990), is 117.97, 124.95 and 115.26 kcal/mol, respectively. The van der Waals volume is 264.93, 273.41, and 291.35 $Å^3$ while the minimal projection area is 32.29, 30.93, and 35.24 $Å^2$, respectively. The minimum z length is 16.83, 16.81, and 17.46 Å, the maximal projection area is 105.83, 107.84, and 113.67 $Å^2$, and the maximum z length is 5.81, 5.59, and 5.48 Å, respectively.

In conclusion, a series of sixteen 2-arylidenehydrazinyl-4-arylthiazole analogues were evaluated for in vivo cytotoxicity using the brine shrimp (A. salina) and for MICs against two Gram-positive bacterial strains (*L. monocytogenes* ATCC 43256 and *E. faecalis* CARS 2011-012) and two Gram-negative bacterial strains (*C. sakazakii* CARS 2012-J-F and *E. coli* CARS 2011-016). The data obtained indicated that compound **3g** with two methoxyl substituents at *ortho*- and *para*-positions of the benzylidene phenyl ring was most cytotoxic to *A. salina* (LC_{50} 54 ppm) and that compound **3h** with an additional bromo substituent at the *para*-position of phenyl ring was the second-most cytotoxic (LC_{50} = 85 ppm). Compound **3i** with three hydroxyl substituents at *para*- and *ortho*-positions of the benzylidene phenyl ring showed potent antibacterial activity against *L. monocytogenes*, *E. faecalis*, and *C. sakazakii* (MIC 50–100 μg mL^{-1}), and compound **3g** exhibited highest antibacterial activity against *E. coli* (MIC 50 μg mL^{-1}). Structure–activity relationships (SAR) studies revealed that moderate electron donating groups (OMe) in the benzylidene phenyl ring are favorable compare to that of more polar groups (OH) to exert brine shrimp cytotoxicity. While structure–antimicrobial activity relationships did not appear to play a significant role. However, the presence of a bromine atom (a bulky and moderate ring deactivating group) at R_5 position greatly reduced both the cytotoxicity and antibacterial activity. Molecular docking studies were performed to investigate interactions between compounds **3c**, **3i**, and **3j** and the active site of *E. coli* FabH receptor. Compound **3i** was found to effectively bind to the active site with a high docking score, indicating it could act as a FabH inhibitor. None of the sixteen analogues violated Lipniski's ROF or

Veber's rule, and thus, they exhibited good drug-likenesses with high drug scores. Additionally, the in silico determined ADME properties of 2-arylidenehydrazinyl-4-arylthiazole analogues suggested they be viewed as potential oral drug candidates. The details of the ligand-receptor and surface interactions of compounds **3c**, **3i,** and **3j** were also analyzed. Accordingly, we conclude that compounds with thiazole frameworks containing the phenyl azomethine amine (Ar–CH=N–NH–) moiety should be considered a basis for the design and development of a new antibacterial FabH inhibitor.

References

Alam MS, Liu L, Lee YE, Lee DU (2011) Synthesis, antibacterial activity and quantum-chemical studies of novel 2-arylidenehydrazinyl-4-arylthiazole analogues. Chem Pharm Bull 59:568–573

Alam MS, Ahmed JU, Lee DU (2014a) Synthesis, antibacterial, antioxidant activity and QSAR studies of novel 2-arylidenehydrazinyl-4-arylthiazole analogues. Chem Pharm Bull 62:1259–1268

Alam MS, Lee DU, Bari ML (2014b) Antibacterial and cytotoxic activities of Schiff base analogues of 4-aminoantipyrine. J Korean Soc Appl Biol Chem 57:613–619

Ban M, Taguchi H, Katsushima T, Takahashi M, Shinoda K, Watanabe A, Tominaga T (1998) Novel antiallergic and antiinflammatory agents. Part I: synthesis and pharmacology of glycolic amide derivatives. Bioorg Med Chem 6:1069–1076

Cheng K, Xue JY, Zhu HL (2013) Design, synthesis and antibacterial activity studies of thiazole derivatives as potent ecKAS III inhibitors. Bioorg Med Chem Lett 23:4235–4238

Chimenti F, Maccioni E, Secci D, Bolasco A, Chimenti P, Granese A, Befani O, Turini P, Alcaro S, Ortuso F, Cardia MC, Distinto S (2007) Selective inhibitory activity against MAO and molecular modeling studies of 2-thiazolylhydrazone derivatives. J Med Chem 50:707–712

Clark RF, Zhang T, Wang X, Wang R, Zhang X, Camp HS, Beutel BA, Sham HL, Gu YJ (2007) Phenoxy thiazole derivatives as potent and selective acetyl-CoA carboxylase 2 inhibitors: modulation of isozyme selectivity by incorporation of phenyl ring substituents. Bioorg Med Chem Lett 17:1961–1965

Cohen A, Verhaeghe P, Crozet MD, Hutter S, Rathelot P, Vanelle P, Azas N (2012) Tandem synthesis and in vitro antiplasmodial evaluation of new naphtho[2,1-d] thiazole derivatives. Eur J Med Chem 55:315–324

Deb PK, Kaur R, Chandrasekaran B, Bala M, Gill D, Kaki VR, Akkinepalli RR, Mailavaram R (2014) Synthesis, anti-inflammatory evaluation, and docking studies of some new thiazole derivatives. Med Chem Res 23:2780–2792

Dewar MJS, Zoebisch EG, Healy EF, Stewart JJP (1985) Development and use of quantum molecular models 75. Comparative tests of theoretical procedures for studying chemical reactions. J Am Chem Soc 107:3902–3909

El-Sabbagh OI, Baraka MM, Ibrahim SM, Pannecouque C, Andrei G, Snoeck R, Balzarini J, Rashad AA (2009) Synthesis and antiviral activity of new pyrazole and thiazole derivatives. Eur J Med Chem 44:3746–3753

Ertl P, Rohde B, Selzer P (2000) Fast calculation of molecular polar surface area (PSA) as a sum of fragment-based contributions and its application to the prediction of drug transport properties. J Med Chem 43:3714–3717

Finney DJ (1978) Statistical method in biological assay, 3rd edn. Charles Griffin and Company, London, p 661

Hartl M, Humpf HU (2000) Toxicity assessment of fumonisins using the brine shrimp (Artemia salina) bioassay. Food Chem Toxicol 38:1097–1102

Heath RJ, Rock CO (1996) Regulation of fatty acid elongation and initiation by acyl-acyl carrier protein in *Escherichia coli*. J Biol Chem 271:1833–1836

Helal MHM, Salem MA, El-Gaby MSA, Aljahdali M (2013) Synthesis and biological evaluation of some novel thiazole compounds as potential anti-inflammatory agents. Eur J Med Chem 65:517–526

Iino T, Hashimoto N, Sasaki K, Ohyama S, Yoshimoto R, Hosaka H, Hasegawa T, Chiba M, Nagata Y, Nishimura JET (2009) Structure–activity relationships of 3,5-disubstituted benzamides as glucokinase activators with potent in vivo efficacy. Bioorg Med Chem 17:3800–3809

Jain A, Pandey V, Ganeshpurkar A, Dubey N, Bansal D (2015) Formulation and characterization of floating microballoons of nizatidine for effective treatment of gastric ulcers in murine model. Drug Deliv 22:306–311

Khandekar SS, Daines RA, Lonsdale JT (2003) Bacterial β-ketoacyl-Acyl carrier protein synthases as targets for antibacterial agents. Curr Protein Pept Sci 4:21–29

Lee JY, Jeong KW, Shin S, Lee JU, Kim Y (2012) Discovery of novel selective inhibitors of Staphylococcus aureus β-ketoacyl acyl carrier protein synthase III. Eur J Med Chem 47:261–269

Li JR, Li DD, Wang RR, Sun J, Dong JJ, Du QR, Fang F, Zhang WM, Zhu HL (2014) Design and synthesis of thiazole derivatives as potent FabH inhibitors with antibacterial activity. Eur J Med Chem 75:438–447

Lipinski CA, Lombardo L, Dominy BW, Feeney PJ (2001) Experimental and computational approaches to estimate solubility and permeability in drug discovery and development settings. Adv Drug Deliv Rev 46:3–26

Lv PC, Wang KR, Yang Y, Mao WJ, Chen J, Xiong J, Zhu HL (2009) Design, synthesis and biological evaluation of novel thiazole derivatives as potent FabH inhibitors. Bioorg Med Chem Lett 19:6750–6754

Mayer BN, Ferrigni NR, Putnam JE, Jacobsen LB, Nichols DE, McLaughlin JL (1982) Brine shrimp: a convenient general bioassay for active plant constituents. Planta Med 45:31–34

Mayo SL, Olafson BD, Goddard WA (1990) DREIDING: a generic force field for molecular simulations. J Phys Chem 94:8897–8909

Mjambili F, Njoroge M, Naran K, Kock CD, Smith PJ, Mizrahi V, Warner D, Chibale K (2014) Synthesis and biological evaluation of 2-aminothiazole derivatives as antimycobacterial and antiplasmodial agents. Bioorg Med Chem Lett 24:560–564

Morris GM, Huey R, Lindstrom W, Sanner MF, Belew RK, Goodsell DS, Olson AJ (2009) AutoDock4 and AutoDockTools4: automated docking with selective receptor flexibility. J Comput Chem 30:2785–2791

Netalkar PP, Netalkar SP, Budagumpi S, Revankar VK (2014) Synthesis, crystal structures and characterization of late first row transition metal complexes derived from benzothiazole core: anti-tuberculosis activity and special emphasis on DNA binding and cleavage property. Eur J Med Chem 79:47–56

Nie Z, Perretta C, Lu J, Su Y, Margosiak S, Gajiwala KS, Cortez J, Nikulin V, Yager KM, Appelt K, Chu S (2005) Structure-based design, synthesis, and study of potent inhibitors of β-ketoacyl-acyl carrier protein synthase III as potential antimicrobial agents. J Med Chem 48:1596–1606

Nishikaku F, Koga Y (1993) Suppression of murine collagen-induced arthritis by treatment with a novel thiazole derivative, SM-8849. Immunopharmacology 25:65–74

Nishina C, Enoki N, Tawata S, Mori A, Kobayashi K, Fukushima M (1987) Antibacterial activity of flavonoids against *Staphylococcus epidermidis*, a skin bacterium. Agric Biol Chem 51:139–143

Novakova I, Subileau EA, Toegel S, Gruber D, Lachmann B, Urban E, Chesne C, Noe CR, Neuhaus W (2014) Transport rankings of nonsteroidal antiinflammatory drugs across blood–brain barrier in vitro models. PLoS ONE 9:e86806

Popsavin M, Torovic L, Svircev M, Kojic V, Bogdanovic G, Popsavin V (2006) Synthesis and antiproliferative activity of two new tiazofurin analogues with 2′-amido functionalities. Bioorg Med Chem Lett 16:2773–2776

Price AC, Choi KH, Heath RJ, Li Z, White SW, Rock CO (2001) Inhibition of β-ketoacyl-acyl carrier protein synthases by thiolactomycin and cerulenin. J Biol Chem 276:6551–6559

Rahmutulla B, Matsushita K, Satoh M, Seimiya M, Tsuchida S, Kubo S, Shimada H, Ohtsuka M, Miyazaki M, Nomura F (2014) Alternative splicing of FBP-interacting repressor coordinates c-Myc, P27Kip1/cyclinE and Ku86/XRCC5 expression as a molecular sensor for bleomycininduced DNA damage pathway. Oncotarget 15:2404–2417

Romagnoli R, Baraldi PG, Brancale A, Ricci A, Hamel E, Bortolozzi R, Basso G, Viola G (2011) Convergent synthesis and biological evaluation of 2-amino-4-(3′,4′,5′-trimethoxyphenyl)-5-aryl thiazoles as microtubule targeting agents. J Med Chem 54:5144–5153

Sadowski J, Kubinyi H (1998) A scoring scheme for discriminating between drugs and nondrugs. J Med Chem 41:3325–3329

Sarojini BK, Krishna BG, Darshanraj CG, Bharath BR, Manjunatha H (2010) Synthesis, characterization, in vitro and molecular docking studies of new 2,5-dichlorothienyl substituted thiazole derivatives for antimicrobial properties. Eur J Med Chem 45:3490–3496

Sevrioukova IF, Poulos TL (2013) Dissecting cytochrome P450 3A4-ligand interactions using ritonavir analogues. Biochemistry 52:4474–4481

Shih MH, Ying KF (2004) Syntheses and evaluation of antioxidant activity of sydnonyl substituted thiazolidinone and thiazoline derivatives. Bioorg Med Chem 12:4633–4643

Shiradkar MR, Akula KC, Dasari V, Baru V, Chiningiri B, Gandhi S, Kaur R (2007) Clubbed thiazoles by MAOS: a novel approach to cyclin-dependent kinase 5/p25 inhibitors as a potential treatment for Alzheimer's disease. Bioorg Med Chem 15:2601–2610

Shoichet BK, McGovern SL, Wei B, Irwin JJ (2002) Lead discovery using molecular docking. Curr Opin Chem Bio 6:439–446

Soares MI, Brito AF, Laranjo M, Paixao JA, Botelho MF, Melo TMVDP (2013) Chiral 6,7-bis(hydroxymethyl)-1*H*,3*H*-pyrrolo[1,2-c]thiazoles with anti-breast cancer properties. Eur J Med Chem 60:254–262

Styrt B, Rocklin RE, Klempner MS (1985) Inhibition of neutrophil superoxide production by fanetizole. Inflammation 9:233–244

Trott O, Olson AJ (2010) AutoDock Vina: improving the speed and accuracy of docking with a new scoring function, efficient optimization, and multithreading. J Comput Chem 31:455–461

Turan-Zitouni G, Ozdemir A, Kaplancikli ZA (2011) Synthesis and antiviral activity of some (3,4-diaryl-3H-thiazol-2-ylidene)pyrimidin-2-yl amine derivatives. Phosphorus–Sulphur–Silicon 186:233–239

Wei L, Cheng J, Meng Y, Ren Y, Deng H, Guo Y (2014) A novel formulation of thiamine dilaurylsulphate and its preservative effect on apple juice and sterilised milk. Food Chem 1:415–422

Weidenbörner M, Chandra Jha H (1993) Antifungal activity of flavonoids and their mixtures against different fungi occurring on grain. Pestic Sci 38:347–351

Yang JM, Chen CC (2004) GEMDOCK: a generic evolutionary method for molecular docking. Proteins 55:288–304

Yang YS, Zhang F, Gao C, Zhang YB, Wang XL, Tang JF, Sun J, Gong HB, Zhu HL (2012) Discovery and modification of sulfur-containing heterocyclic pyrazolone derivatives as potential novel class of β -ketoacyl-acyl carrier protein synthase III (FabH) inhibitors. Bioorg Med Chem Lett 22:4619–4624

Ye J, Liu Q, Wang C, Meng Q, Sun H, Peng J, Ma X, Liu K (2013) Benzylpenicillin inhibits the renal excretion of acyclovir by OAT1 and OAT3. Pharmacol Rep 65:505–512

Zablotskaya A, Segal I, Geronikaki A, Tatiana E, Belyakov S, Petrova M, Shestakova I, Zvejniece L, Nikolajeva V (2013) Synthesis, physicochemical characterization, cytotoxicity, antimicrobial, antiinflammatory and psychotropic activity of new N-[1,3-(benzo)thiazol-2-yl]-ω-[3,4-dihydroisoquinolin-2(1*H*)-yl]alkanamides. Eur J Med Chem 70:846–856

Zhang MQ, Wilkinson B (2007) Drug discovery beyond the 'rule-of-five'. Curr Opin Biotechnol 18:478–488

Zhang WT, Ruan JL, Wu PF, Jiang FC, Zhang LN, Fang W, Chen XL, Wang Y, Cao BS, Chen GY, Zhu YJ, Gu J, Chen JG (2009) Design, synthesis, and cytoprotective effect of 2-aminothiazole analogues as potent poly(ADP-Ribose) polymerase-1 inhibitors. J Med Chem 52:718–725